Incidence of hyperaccumulation and tissue-level distribution of manganese, cobalt and zinc in the genus Gossia (Myrtaceae)

Farida Abubakari, Philip Nti Nkrumah, Denise Fernando, Gillian Brown, Peter Erskine, Guillaume Echevarria, Antony van Der Ent

Incidence of hyperaccumulation and tissue-level distribution of manganese, cobalt and zinc in the genus *Gossia* (Myrtaceae)

Farida Abubakari[1], Philip Nti Nkrumah[1], Denise R. Fernando[2], Gillian K. Brown[3], Peter D. Erskine[1], Guillaume Echevarria[4], Antony van der Ent[1,4*]

[1]Centre for Mined Land Rehabilitation, Sustainable Minerals Institute, The University of Queensland, Australia.

[2]Department of Ecology, Environment and Evolution, La Trobe University, Australia.

[3]Department of Environment and Science, Queensland Herbarium, Toowong, Australia.

[4]Université de Lorraine – INRA, Laboratoire Sols et Environnement, UMR 1120, France.

*corresponding author: a.vanderent@uq.edu.au

Summary

- The rare phenomenon of plant manganese (Mn) hyperaccumulation within the Australian flora has previously been detected in the field, which suggested that the tree genus *Gossia* (Myrtaceae) might contain new Mn hyperaccumulators.
- We conducted the first growth experiment on *Gossia* using a multi-factorial dosing trial to assess Mn, cobalt (Co) and zinc (Zn) (hyper)accumulation patterns in selected *Gossia* species (*G. fragrantissima* and *G. punctata*) after a systematic assessment of elemental profiles on all holdings of the genus *Gossia* at the Queensland Herbarium using handheld X-ray fluorescence spectroscopy. We then conducted detailed *in situ* analyses of these elemental distributions at the macro (organ) and micro (cellular) levels with laboratory- and synchrotron-based X-ray Fluorescence Microscopy (XFM).
- *Gossia pubiflora* and *G. hillii* were newly discovered to be Mn hyperaccumulator plants. In the dosing trial, *G. fragrantissima* accumulated 17 400 μg g^{-1} Mn, 545 μg g^{-1} Co and 13 000 μg g^{-1} Zn. The laboratory based XFM revealed distinct patterns of accumulation of Co, Mn and Zn in *G. fragrantissima*, while the synchrotron XFM showed their localization in foliar epidermal, and in the cortex and phloem of roots.
- This study combined novel analytical approaches with controlled experimentation to examine metal hyperaccumulation in slow-growing woody species, thereby enabling insight into the phenomenon not possible through field studies.

Graphical abstract

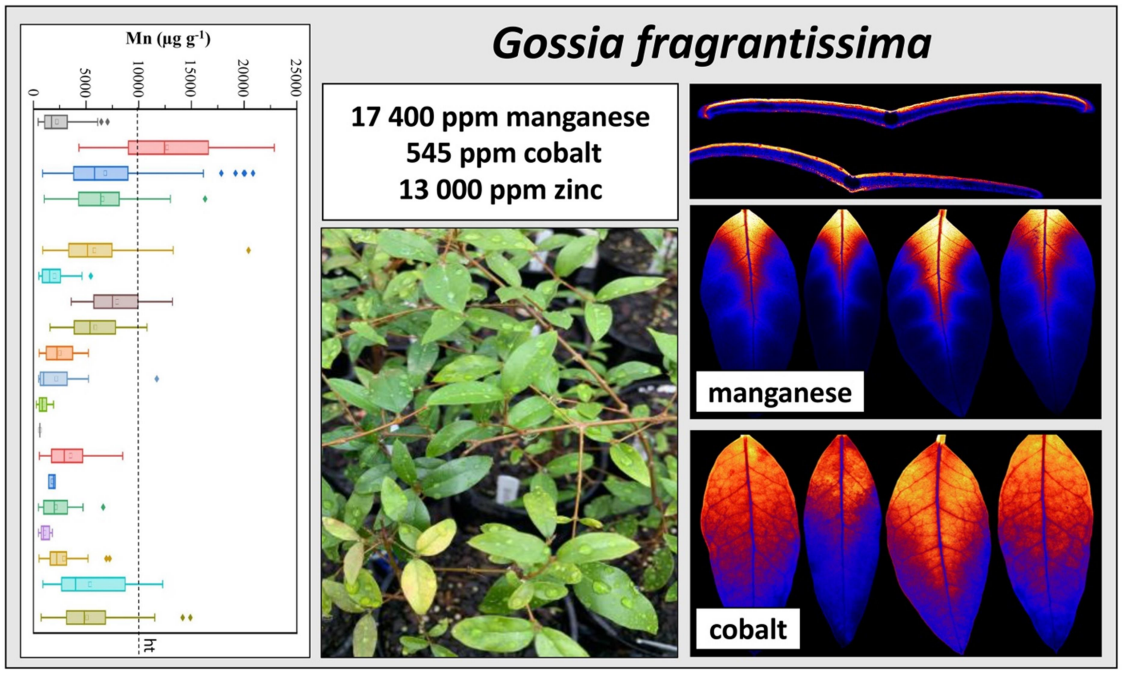

This study combined novel analytical approaches with controlled experimentation to examine metal hyperaccumulation in slow-growing woody species, thereby enabling insight into the phenomenon not possible through field studies. This study highlights a new era of hyperaccumulator plants discovery, with added advantage of identifying species of interest for further ecophysiological and elemental distribution investigations.

Key words: elemental distribution, hyperaccumulator, *Gossia fragrantissima*, *Gossia punctata*, trace element, metal homeostasis

INTRODUCTION

Hyperaccumulators are unusual plants that are able to accumulate extraordinarily high concentrations of specific trace elements into their shoots.[1-3] They achieve this through enhanced uptake and translocation mechanisms.[4, 5] Hyperaccumulation thresholds have been set for different elements, including 300 μg g^{-1} for Co, 3000 μg g^{-1} for Zn and 10 000 μg g^{-1} dry weight for Mn.[3] The hyperaccumulation phenomenon is rare (exhibited by <0.2% of angiosperms) with ~70% of the known 700 hyperaccumulator species recorded for Ni. [2, 6] Their occurrence is primarily on substrates enriched in the elements that they hyperaccumulate, most commonly ultramafic soils which are high in Ni, Co and Mn. [7]

Manganese, a micronutrient essential for plant growth and function, is transported *in planta* in its free divalent form Mn^{2+}. [8, 9] Plant tissue Mn is usually around 50–800 μg g^{-1} dry weight, sometimes exceeds 1000 μg g^{-1} in species growing on normal soils[10, 11], and up to 1000–7000 μg g^{-1} in plants growing on Mn-enriched substrates.[12] Deficiency symptoms may occur at foliar concentrations less than 10 μg g^{-1} whilst toxicity symptoms typically appear at 1000–12 000 μg g^{-1} depending on the species.[12] The solubility of Mn (*i.e.* in Mn^{2+} state) increases with increase in soil acidity and extreme climatic conditions which give rise to soil waterlogging, heating and drying[13-15] as well as the activities of aerobic and anaerobic microorganisms. Higher valency states of Mn of +4 and +3 are insoluble.[16] However, the ability of Mn to form anionic complexes (MnO^-_4) and organic ligands can increase its solubility in the alkaline pH range.[17, 18] Plants growing in alkaline soils take up Mn by root exudate production in the rhizosphere, for example in Proteaceous cluster roots.[19-22] A Mn-citrate chelate is suspected in species that hyperaccumulate Mn through exuding large quantities of carbocyclic acids, such as *Phytolacca americana*. [23]

The global database for plants that hyperaccumulate metal and metalloid trace elements reported 42 known Mn hyperaccumulator species[6], with majority restricted over eastern Australia and New Caledonia.[1, 24, 25] Manganese hyperaccumulation in New Caledonia was discovered in the 1970's [26, 27], and studies on Mn hyperaccumulator plants in Australia are more recent.[28] Recently, the use of handheld X-ray Fluorescence (XRF) instruments to non-destructively perform systematic quantitative assessments of the elemental composition of herbarium specimens[29] has led to dramatic increases in the number of known hyperaccumulator plants globally. Even in the well-studied flora of New Caledonia, this approach led to an increase of the known Mn hyperaccumulators from 11 to 74 Mn hyperaccumulator taxa.[30] New discoveries of Mn hyperaccumulators in Malaysia and Papua New Guinea further support existing hypotheses that plant-Mn hyperaccumulation in the Western Pacific and Southeast Asia is likely widespread.[31-34] Most Mn hyperaccumulator species have been found in the families of Apocynaceae, Celastraceae, Clusiaceae, Myrtaceae and Proteaceae.[24, 35, 36]

The genus *Gossia* (Myrtaceae) contains 20 exceptionally Mn-accumulating species in eastern Australian rainforests, on soils derived from acid volcanic substrates (primarily andesite, basalt, granite, and ignimbrite) as well as laterites, meta-sediments and sandstones.[1, 24, 25, 37] Unlike New Caledonian *Gossia* species, the ones in the Australian flora occur less frequently on ultramafic soils, except for *Gossia bidwillii*.[37] *Gossia bidwillii* was the first Australian Mn hyperaccumulator discovered[28], instigating further research on Mn hyperaccumulation in various species of *Gossia* in Australia.[25, 38-40] *Gossia fragrantissima* was shown via field studies and analysis of herbarium specimens to accumulate unusually high Zn, Co and Ni concentrations in addition to Mn.[25, 40] Whereas several *Gossia* species in the Australian flora

are strong Mn accumulators, there are other species in the genus that exhibit weak Mn accumulating capacity. For example, separate herbarium and field data are in agreement that *G. punctata* is not a Mn (hyper) accumulator.[25, 40]

Previous hyperaccumulation studies on *Gossia* have mainly focused on investigating the phylogeny, biogeography and bulk leaf-accumulation[37] as well as prospecting for new Mn hyperaccumulators.[25] However, little is known about the hyperaccumulation of Co and Zn in this genus. X-ray elemental mapping techniques can play an important role in answering questions about plant metal homeostasis at many levels from the rhizosphere interface, to uptake pathways in the roots and shoot.[33] The use of the Proton Induced X-ray Emission (PIXE) analysis has revealed Mn in addition to Ni and Co in a freeze-dried leaf of *G. fragrantissima* to be localized in palisade mesophyll cell vacuoles whereas Zn is primarily located in the upper epidermis.[40] X-ray Florescence Microscopy (XFM) is a powerful tool for elucidating elemental distribution in hydrated plant organs and tissues (hydrated materials) and could provide useful information to complement previous reports. In particular, the co-accumulation of Mn, Co and Zn raises the question whether the three elements follow the same pathways in the plant - from selective root uptake to accumulation in storage tissues. It also raises questions about competition between the three elements. These can be best addressed *via* controlled experiments to direct future investigations into molecular mechanisms that underpin metal co-accumulation. To date, no study has investigated the elemental distribution in fresh plant organs and tissues of *G. fragrantissima*. Therefore, this study seeks to (i) systematically assess the incidence of Mn, Co and Zn accumulation in the genus *Gossia* in Australia through herbarium XRF scanning, (ii) investigate the (hyper)accumulation of *G. fragrantissima* under controlled conditions in a multi-factorial randomised block design Mn, Co and Zn dosing trial, and contrast it with the non-

hyperaccumulator *G. punctata,* and (iii) finally use laboratory and synchrotron X-ray Florescence Microscopy (XFM) to determine the *in situ* distribution of Mn, Co and Zn in hydrated plant organs and tissues of *G. fragrantissima* and *G. punctata.*

MATERIALS AND METHODS

Herbarium XRF assessment of hyperaccumulation

The use of handheld X-ray fluorescence (XRF) instruments is a non-destructive and effective method for the systematic quantitative assessment of hyperaccumulation in vast numbers of herbarium specimens [29]. It has the ability to measure a range of different elements, including the transition elements Ni, Co, Mn and Zn. The Thermo Fisher Scientific Niton XL3t 950 GOLDD+ analyser uses a miniaturised X-ray tube (Ag anode, 6–50 kV, 0–200 μA max) as its excitation source. The X-ray tube irradiates the sample with high-energy X-rays, which excite fluorescent (characteristic) X-rays in the sample. These fluorescent X-rays are detected and quantified with a large 20 mm^2 Silicon Drift Detector and it has practical detection limit for plant material samples of the order of >300 $\mu g\ g^{-1}$ depending on the element. The XRF analysis was undertaken on a sheet of 'herbarium cardboard' on a pure titanium plate (~99.995%, 2 mm thick × 10 × 10 cm) to provide a uniform background and block transmitted X-rays. The XRF analysis used the 'Soils Mode' in the 'Main filter' configuration for 30s duration.

Calibration of the raw XRF data was achieved using an empirical approach. Two hundred and twenty-one (221) samples from the Herbarium of New Caledonia (NOU) were intentionally chosen to cover a very wide range ('normal' to hyperaccumulation – see below) of Mn, Co, Ni and Zn values and a 1 cm^2 area destructively excised from each specimen. This

fragment was analysed by XRF, then weighed and pre-digested in 1 mL 70% HNO_3 and subsequently digested in a microwave oven (Milestone Start D) at 125°C for 2 hours and diluted to 10 mL with ultra-pure water (Millipore 18.2 MΩ·cm at 25°C) before analysis with Inductively coupled plasma atomic emission spectroscopy (ICP-AES) with a Thermo Scientific iCAP 7400 instrument for Mn, Co, Ni, Zn in radial and axial modes depending on the element and analyte concentration. The elements were calibrated with a 4-point curve covering analyte ranges in the samples. In-line internal addition standardization using yttrium was used to compensate for matrix-based interferences. Quality controls included matrix blanks, certified reference material (Sigma-Aldrich Periodic Table mix 1 for ICP TraceCERT®, 33 elements, 10 mg L^{-1} in HNO_3).

The XRF analysis was undertaken at the Queensland Herbarium (BRI) in Brisbane. The Queensland Herbarium contains over 880 000 specimens and 98.8% of the collection is databased. Nine hundred and sixty one specimens of the following 20 species of *Gossia* specimens, originating from Queensland, were scanned: (*Gossia acmenoides, G. bamagensis, G. bidwillii, G. byrnesii, G. dallachiana, G. floribunda, G. fragrantissima, G. gonoclada, G. grayi, G. hillii, G. inophloia, G. lewisensis, G. lucida, G. macilwraithensis, G. myrsinocarpa, G. pubiflora, G. punctata, G. retusa, G. sankowskyorum, and G. shepherdii*).

Gossia species studied in the metal dosing trial

Gossia fragrantissima (F. Muell. ex Benth.) N.Snow & Guymer (Myrtaceae), sweet myrtle or small-leaved myrtle is a shrub or small tree which grows in sub-tropical rainforest on basalt-derived soils in south-east Queensland and in north-east New South Wales, located south to the Richmond River. [41, 42] It grows to a height of about 4–10 m tall with rough, brown,

fissured bark; young shoots sparsely hairy with short brown hairs. The leaves are small and glossy with a tiny point at the apex and paired on the stem [42].

Gossia punctata N. Snow & Guymer (Myrtaceae) is a small tree which grows in dry rainforest on dry skeletal soil mainly on the inland coastal ranges; north from the Nymboida River. It grows to a height of 15 m tall with grey scaly bark; young shoots are finely pubescent and glabrous with age. The leaf lamina is elliptic, apex acuminate, lower surface glabrous, oil glands conspicuous on lower surface with petiole of 1–2 m long. The flowers are solitary and hypanthium glabrous or finely pubescent [41].

Plant dosing treatments

The two species studied (*G. fragrantissima* and *G. punctata*) were obtained from Burringbar Rainforest Nursery and grown from seed (Burringbar Road, Upper Burringbar, NSW). The provenance of the seeds was a mature tree growing near Burringbar originating from the native population of *G. fragrantissima* in the Tweed Shire. Similarly, for *G. punctata* the provenance of the seeds was from a population near Burringbar. The plants were cultivated in a temperature and humidity-controlled glasshouse with 20ºC and 80% relative humidity (RH) and 1600 µM m^{-2} s^{-1} PAR flux density for ~13 hrs, at the Central Glasshouse Services (CGS) in St Lucia at The University of Queensland, Australia. After three weeks, the plants were transferred into 15 cm pots containing a ratio of 9:1 mixture of composted pine bark (aggregate size, 5–10 mm) and Coco Peat (Bassett Barks Pty Ltd, Queensland, Australia). The media was mixed with low-level fertilizers and other augments consisting (per m^3) of 1.2 kg Yates Flowtrace, 1 kg iron sulphate heptahydrate ($FeO_4SO_4 \cdot 7H_2O$), 0.1 kg superphosphate ($Ca(H_2PO_4)_2$), 1.5 kg gypsum ($CaSO_4$) and 1.5 kg dolomite ($CaMg(CO_3)_2$). The composition of the Flowtrace was 24 wt% iron (Fe) as $FeSO_4$, 14 wt% sulfur (S) as SO_4, 0.75 wt% copper

(Cu) as $CuSO_4$, 0.5 wt% manganese (Mn) as $MnSO_4$, 0.2 wt% zinc (Zn) as $ZnSO_4$, 0.04 wt% molybdenum (Mo) as Na_2MoO_4, 0.033 wt% boron (B) as $Na_2B_4O_7$ and also contains zeolite, to ensure flowability (Yates Australia, Padstow, NSW, Australia). Soluble Mn, Co and Zn were applied to the plants in a multi-factorial randomised block design. The applied treatments were the control (T1), and soils with final concentrations of Mn^{2+}, Co^{2+} and Zn^{2+} of 200 μg g^{-1}, 500 μg g^{-1}, 1000 μg g^{-1} and combination of Co+Mn+Zn respectively yielding a total of 13 experimental groups. Each treatment was administered monthly as aqueous $MnSO_4.H_2O$, $CoSO_4.7H_2O$ and $ZnSO_4.7H_2O$ solutions for a period of 12 months; a similar volume of water was added to the control each time. The individual pots were placed on saucers and hand watered daily to field capacity to prevent loss of treatment solutions. In total there were 78 experimental pots of all factorial combinations of two species and thirteen substrate Mn, Co and Zn solutions replicated three times.

Chemical analysis of soil and plant samples

After harvesting, the soil was extracted in each pot and emptied into respective plastic bags. The soil samples were further air-dried, sieved and 50 g was weighed from each pot. Soil sub-samples (~300 mg) were digested using 9 mL 70% HNO_3 and 3 mL 37% HCl per sample in a digestion microwave (Milestone Start D) for a program of 1.5 hours and diluted to 40 mL with ultrapure water before analysis to obtain pseudo-total elemental concentrations. Soil pH was obtained in a 1:2.5 soil:water mixture after 2 hr shaking. Exchangeable trace elements were extracted in 0.1 M $Sr(NO_3)_2$ at a soil:solution ratio of 1:4 (10 gram soil with 40 mL solution) and 2 hr shaking time was adapted from Kukier and Chaney.[43] As a means of estimating potentially phytoavailable trace elements, the DTPA-extractant was used according to Becquer et al. [44] which was adapted from the original method by Lindsay and

Norvell[45], with the following modifications: excluding TEA, adjusted at pH 5.3, 5 g soil with 25 mL extractant, and an extraction time of one hr.

The plant material samples were oven-dried at 60°C for three days. Each sample was weighed, ground to fine powder and digested using 4 mL HNO_3 (70%) in a microwave oven (Milestone Start D) for a 45-minute programme and diluted to 45 mL with ultrapure water (Millipore 18.2 MΩ·cm at 25°C) before analysis for macro-elements (Na, Mg, K, Ca) and trace-elements (Mn, Co, Zn) in radial and axial modes depending on the element and expected analyte concentration. All elements were calibrated with a 4-point curve covering analyte ranges in the samples. In-line internal addition standardization using yttrium was used to compensate for matrix-based interferences. Quality controls included matrix blanks, certified reference material (Sigma-Aldrich Periodic Table mix 1 for ICP TraceCERT®, 33 elements, 10 mg L^{-1} in HNO_3), Standard Reference Material (NIST Apple 1515 digested with HNO_3), and internal reference materials.

Desktop micro-X-ray Fluorescence Microscopy (XFM)

Freshly detached branchlets of *G. fragrantissima* and *G. punctata* from the Mn1000Co1000Zn1000 treatment were used for the microXRF scanning. The UQ microXRF facility contains a modified IXRF ATLAS X system, mounting two 50W X-ray sources fitted with polycapillary focussing optics: XOS microfocus Mo-target tube producing 17.4 keV X-rays (flux of 2.2×10^8 ph s^{-1}) focussing to 25 µm and a Rh-target tube producing 20.2 keV (flux of 1.0×10^7 ph s^{-1}) focussing to 5 µm. The system is fitted with two silicon drift detectors of 150 mm^2 coupled unit. Samples for analysis were mounted between two sheets of Ultralene thin (4 µm) film stretched over a Perspex frame. Measurements were conducted at room temperature (~20°C), using the Mo 25 µm X-ray source at a 40 kV, 1000 uA, with a

rise time of 0.25 µs and a per-pixel dwell of 100 ms. The tight sandwich-like mounting of the sample was designed to optimise retention of its fresh hydrated state, with analysis completed within 10 minutes after excision. The risk of radiation-induced damage, particularly to fresh hydrated samples was avoided/minimised here by choosing appropriate operating conditions, *i.e.,* a source flux of 2.2×10^8 photons s^{-1} in a 25 µm beam spot at a maximum dwell of 100 ms, resulting in a deposited radiation dose of just 6.6 Gy.

Synchrotron micro-X-ray Fluorescence Microscopy (XFM)

The X-ray fluorescence microscopy (XFM) beamline at the Australian Synchrotron employs a Si(111) monochromator and a pair of Kirkpatrick-Baez mirrors to deliver X-rays onto the specimen with fluorescent X-rays collected in a backscatter geometry using the 384-element Maia detector system.[46] The Maia detector uses a large detector array to maximise detected signal and count-rates for efficient imaging. Maia enables high overall count-rates and uses an annular detector geometry, where the beam passes through the detector and strikes the sample at normal incidence[47, 48] to maximise detected signal and hence reduce the dose and potential damage to analysed specimens.[49] The samples were hand cut with a stainless-steel razor blade ('dry knife'), mounted between two sheets of 4 µm Ultralene thin film in a tight sandwich to limit evaporation, and analysed within 5 minutes after excision. The hydrated samples were mounted between two sheets of Ultralene thin film (4 µm) stretched over a Perspex frame magnetically attached to the *x-y* motion stage at atmospheric temperature (~20°C). First, a quick 'survey scan' was conducted to allow for the selection of the appropriate portion of the sample. For the survey scan, the resolution was 50–100 µm with a dwell of 1–2 ms and generally took ca. 5 min to complete. After that a 'detailed scan' was conducted, with a resolution of 2–10 µm and a dwell of 8–20 ms and generally took ca. 100

min, depending on the mapped area. For the whole experiment, an incident energy of 15.8 keV was used in order to excite the highest *Z* element of interest (*i.e.,* Zn).

Statistical analyses

The matching XRF and ICP-AES data was used to obtain calibration curves. The apparent limits of detection (LOD) for Ni, Co and were estimated by visual inspection of the log-transformed regression models of the XRF data against corresponding ICP-AES measurements and set at XRF values: 107 μg g^{-1} for Ni (range 107–113 987, n = 149), 426 μg g^{-1} for Co (372–9532, n = 50), 455 μg g^{-1} for Mn (455–176 396, n = 159) and 27 μg g^{-1} for Zn (range 27–1238, n = 117). The residuals *vs.* fitted values were inspected for each linear regression analysis, and outliers (± 3 SD of the residual) were identified and removed. Secondary linear regression models were then derived after the samples with XRF values below the limit of detection were removed. The regression models (y = calculated ICP-AES; x = measured XRF) are: Ni: $y = 0.2351x^{1.0969}$ (R^2 0.98), Mn $y = 0.7869x^{0.9165}$ (R^2 0.98), Co: $y = 0.429x^{0.9809}$ (R^2 0.92), and Zn: $y = 0.3766x^{1.1259}$ (R^2 0.88).

Statistical analyses were performed using R version 3.6.1 (2019-07-05) and Microsoft Excel 2016. The concentration of Co, Mn and Zn are presented as boxplots. The concentration of elements given in tables represents mean ± SE of three replicate plants. The mean ± standard error of mean was determined using descriptive analysis tool, and the two-way ANOVA with confidence level of 95% in the Analysis Toolpak in Microsoft Excel 2016 was used to analyse the differences between treatment levels, species and their interaction (treatment levels * species) and their *P* values of significance were presented. The mean ± standard error followed by the same letter are not significantly different ($p < 0.05$) as stated by Duncan-Waller K-ratio t-test.

The XRF spectra on the UQ microXRF facility were acquired in mapping mode using the instrument control package, Iridium (IXRF systems), and then imported into the GeoPIXE software package version 7.5s (beta). The XRF spectra were subsequently fitted using the Dynamic Analysis method.[50-53] This method generates elemental images, which are line overlap-resolved, and in with the Mo-tube Bremsstrahlung background has been subtracted. The sample matrix was modelled using an empirical formula for hydrated plant material samples with the composition $C_{7.3}O_{33}H_{59}N_{0.7}S_{0.8}$ with a density of 0.90 g cm^{-3} and a thickness of 500 µm, overlaid by one layer of Ultralene ($C_{14}H_{10}O_4$, 6 µm, density of 1.36 g cm^{-3}).

RESULTS

Systematic assessment of Mn, Co and Zn accumulation in the genus *Gossia*

Systematic assessment of Mn, Co and Zn accumulation on all holdings of the genus *Gossia* undertaken at the Queensland Herbarium using handheld XRF is shown in Fig. 1. The results show that *G. bamagensis* is an exceptional Mn hyperaccumulator with concentrations reaching up to 22 900 µg g^{-1} (mean is 11 800 µg g^{-1}, n = 14). Other species with concentrations above the Mn hyperaccumulation threshold were *G. bidwillii* (880–20 900 µg g^{-1}, mean 6800 µg g^{-1}, n = 134), *G. fragrantissima* (3600–13 200 µg g^{-1}, mean 7800 µg g^{-1}, n = 10), *G. dallachiana* (890–20 400 µg g^{-1}, mean 5800 µg g^{-1}, n = 41), *G. gonoclada* (460–10 800 µg g^{-1}, mean 5580 µg g^{-1}, n = 21), *G. pubiflora* (1030–16 300 µg g^{-1}, mean 6570 µg g^{-1}, n = 24), *G. sankowskyorum* (480–12 300 µg g^{-1}, mean 5170 µg g^{-1} Mn, n = 26) and *G. shepherdii* (470–14 800 µg g^{-1}, mean 4640 µg g^{-1}, n = 44) (Fig. 1).

The only multi-element hyperaccumulator was *G. fragrantissima* which in addition to Mn, accumulates Co and Zn with concentrations of 485 μg g^{-1} Co and up to 3900 μg g^{-1} Zn, respectively (Fig. 1). *Gossia pubiflora* displayed remarkable Zn accumulating capacity, with the highest concentration of 1590 μg g^{-1} Zn, though below the Zn hyperaccumulation threshold level (Fig. 1).

Bulk elemental concentrations in plant tissues of *Gossia* from the dosing trial

The multi-factorial randomised block design dosing trial for the uptake of Mn, Co and Zn in *G. fragrantissima* and *G. punctata* lasted for 12 months during which time the plants grew about double in size. No signs of toxicity were observed in *G. fragrantissima*. However, in *G. punctata* visible signs of chlorosis, miniature leaves and brown speckles in older leaves were observed at the highest treatment levels of Mn, Co and Zn and Co+Mn+Zn. The results of the bulk elemental concentrations determined in young, old leaves and twigs of *G. fragrantissima* and *G. punctata* after exposure to single treatments of Co, Mn and Zn and their combinations (Co+Mn+Zn) at different levels are shown in Figs 2 and 3, Tables S1–S4. Mean Mn concentrations in *G. fragrantissima* were 16 500 μg g^{-1} (SE ± 875 μg g^{-1}) in young leaves and 17 400 μg g^{-1} (SE ± 4580 μg g^{-1} Mn) in old leaves which is more than 1.5-fold the Mn hyperaccumulation threshold at the 1000 μg Mn g^{-1} treatment level. Twigs, however, contained on average approximately four times lower Mn concentrations than young and old leaves at the same treatment level (Fig. 2, Table S2). The concentrations of Mn at the 500 μg Mn g^{-1} treatment level were also relatively high in young leaves (5210 ± 405 μg g^{-1}) and old leaves (7060 ± 2200 μg g^{-1}) of *G. fragrantissima* than in twigs (1890 ± 280 μg g^{-1}). The Mn concentration in the various plant fractions in the 500 μg Mn g^{-1} treatment level were relatively higher compared to the 200 μg Mn g^{-1} treatment level and the control. The concentrations of Co in young leaves, old leaves and twigs were significantly above the Co

hyperaccumulation threshold at the 1000 µg Co g^{-1} treatment level with mean values of 348 µg g^{-1} (SE ± 150 µg g^{-1} Co), 525 µg g^{-1} (SE ± 405 µg g^{-1} Co) and 345 µg g^{-1} (SE ± 115 µg g^{-1}), respectively. On the other hand, the 500 µg Co g^{-1} treatment level had significantly higher Co concentrations above the Co hyperaccumulation threshold in old leaves (320 ± 85.0 µg g^{-1} Co) compared to the young leaves (225 ± 8.00 µg g^{-1} Co) and twigs (205 ± 40 µg g^{-1} Co) (Fig. 2, Table S1).

The concentrations of Zn in *G. fragrantissima* in the 500 µg Zn g^{-1} and 1000 µg Zn g^{-1} treatment levels were remarkable, with values in young and old leaves ~3-fold and ~4-fold higher than the hyperaccumulation threshold for Zn, respectively (Fig. 2, Table S3). The mean Zn concentrations in young and old leaves of *G. fragrantissima* at the 200 µg Zn g^{-1} treatment level were also significantly above the Zn hyperaccumulation threshold compared to the control (Fig. 2, Table S3). The highest mean Zn concentrations was recorded at the highest level of treatments in old leaves, with mean concentrations of 13 000 µg g^{-1} (SE ± 3840 µg g^{-1}), followed by young leaves (11 400 ± 2500 µg g^{-1}) and twigs (2930 ± 665 µg g^{-1}).

Interestingly, the combination of Co+Mn+Zn at all levels of treatments, led to a significant reduction in Zn concentrations in young, old leaves and twigs but an increase in the mean concentrations of Co and Mn in *G. fragrantissima* (Fig. 3, Table S4). However, in the single Co and Zn treatments, Mn concentrations in young leaves, old leaves and twigs of *G. fragrantissima* increased with increasing treatment levels (Fig 2. Tables S2 and S3). Cobalt at the 200 µg Co g^{-1}, 500 µg Co g^{-1} and 1000 µg Co g^{-1} treatment levels in old leaves were more than 2-fold relative to the Co hyperaccumulation threshold. In the young leaves, the mean concentration of Co exceeded the hyperaccumulation threshold at all treatment levels, reaching 3-fold higher in the highest treatment level. The concentration of Mn at the 1000 µg

Co g^{-1} treatment level in the old leaves was above the Mn hyperaccumulation threshold (Fig. 3, Table S4). The mean ± SE concentrations of Co, Mn and Zn in young leaves at the highest level of treatments were 1040 ± 235 µg g^{-1}, 2170 ± 360 µg g^{-1} and 760 ± 175 µg g^{-1}, respectively. In old leaves, relatively higher concentrations of Co (1140 ± 35 µg g^{-1}), Mn (10 900 ±1380 µg g^{-1}) and Zn (965 ± 460 µg g^{-1}) were measured. The twigs had 840 ± 170 µg Co g^{-1}, 4440 ± 590 µg Mn g^{-1} and 605 ± 90 µg Zn g^{-1}.

In contrast to *G. fragrantissima*, the concentrations of Co, Mn and Zn in young leaves, old leaves and twigs of the non-hyperaccumulator *G. punctata* were below the 300 µg g^{-1}, 10 000 µg g^{-1}, and 3000 µg g^{-1} hyperaccumulation threshold of Co, Mn and Zn, respectively, even at the highest treatment level (Fig. 2 and 3, Tables S1–S4). The concentrations of Co, Mn and Zn of *G. punctata* in the combined treatment (Co+Mn+Zn) were 155 ± 25 µg Co g^{-1}, 590 ± 105 µg Mn g^{-1} and 210 ± 10 µg Zn g^{-1} in young leaves, whereas the old leaves had 180 ± 40 µg Co g^{-1}, 1380 ± 340 µg Mn g^{-1} and 250 ± 35 µg Zn g^{-1}. The twigs had 155 ± 20 µg Co g^{-1}, 325 ± 80 µg Mn g^{-1} and 90 ± 20 µg Zn g^{-1}. Whereas the young leaves, old leaves and twigs of *G. fragrantissima* had significantly higher concentrations of Mn, Co and Zn than *G. punctata*, the concentrations of Ca, Mg, Na and K were lower in the former than the latter (Figs. 2 and 3, Tables S1–S4). The concentrations of Ca, Mg, Na and K increase with decreasing Mn in the young leaves, old leaves and twigs of *G. punctata* in all treatments.

Pot soil properties in the dosing trial

The results of the pH, DTPA- and $Sr(NO_3)_2$-extractable concentrations in soils of *G. fragrantissima* and *G. punctata* at harvest are shown in Table S5. There were no significant differences in the soil pH in the control, 200 µg Zn g^{-1} and 1000 µg Zn g^{-1} treatment levels between *G. fragrantissima* and *G. punctata*. The DTPA extractable concentrations of Mn

and Zn were ~4- and ~3-fold, respectively, at the 1000-treatment level, ~3 fold each at 500-treatment level and 2-fold each at the 200-treatment level, higher compared to the control.

Desktop XFM analysis of *G. fragrantissima* and *G. punctata*

Whole live leaves from the highest-level dosing treatments were used for elemental mapping using the UQ microXRF facility as shown in Figs. 4 and 5 for *G. fragrantissima* and Fig. 6 for *G. punctata*. In the whole leaves of *G. fragrantissima*, Mn is mainly localised at the apex of the leaf margin and petiole loading down to the leaf bases but more in old leaves than young leaves (Figs. 4 and 5). The concentration of Ca mirrors that of Mn at the leaf apex with strong enrichment in the leaf margins and petiole and with enrichment in the veins and midrib and at the lower base of the stem in old than in young leaves (Figs. 4 and 5). Cobalt distribution mirrors that of K with enrichment in the leaf margin, stipule, and lateral veins but Co is low in the midrib (Figs. 4 and 5). Zinc is strongly enriched in the leaf margins, and towards the leaf apex and stem (Figs. 4 and 5). However, in *G. punctata*, although the distribution of Mn mirrors that of Ca, but high enrichment of Ca than Mn can be seen throughout the leaf blade of young and in stem than in old leaves (Fig. 6). The distribution of Zn is in the stem and petioles and with small circular patches of 'dots' concentration of Co and Zn visible in young leaf margins but their concentrations (*i.e.*, Co and Zn) in *G. punctata* is low as compared to that in *G. fragrantissima* (Figs. 4 and 5).

Synchrotron XFM analysis of *G. fragrantissima*

The results of the elemental distribution in leaf and root cross-sections as well as in whole leaf of *G. fragrantissima* using the X-ray florescence microscopy (XFM) beamline are shown in Figs. 7, 8 and 9, respectively. In the leaf cross section, there is a strong enrichment of Ca, Co, Mn, Ni, K and Zn in the lower and upper epidermis, and in the cuticle, collenchyma and

parenchyma but low in the xylem and phloem (Fig. 7). Whereas in the root cross section, the concentration of Co, K, Mn and Zn are predominantly high in the cortex and phloem, but low in the epidermis and xylem (Fig. 9). In the whole leaf of *G. fragrantissima*, the distribution of Co mirrors that of Ni, Mn and Zn with strong enrichment at the leaf bases (Fig. 8). In contrast, K distribution tends to be concentrated (more than half) at the upper part of the leaf (Fig. 8). Calcium is strongly enriched at the leaf margin, midrib and veins (Fig. 8).

DISCUSSION

This study assessed 20 species of *Gossia* for the occurrence of Mn, Co and Zn hyperaccumulation. As a result, eight were found to be Mn hyperaccumulators and can be termed 'hypermanganesophores' (species with >10 000 μg g^{-1} Mn in foliage).[54] *Gossia hillii* could also be termed as such, although contains Mn from 500 to 5240 μg g^{-1} but has an outlier of up to 11 700 μg g^{-1} Mn (Fig. 1). *Gossia punctata*, G. *byrnesii*, *G. inophloia*, *G. lewisensis*, *G. macilwraithensis*, *G. lucida*, *G. acmenoides*, *G. floribunda*, *G. retusa* and *G. myrsinocarpa* did not hyperaccumulate Mn. However, three of these Mn non-hyperaccumulators species (G. *inophloia*, *G. lewisensis* and *G. macilwraithensis*) including *G. hillii* have previously been reported by Fernando et al.[25] to accumulate high concentrations of Al. *Gossia bamagensis* was the strongest Mn hyperaccumulator plant among all the *Gossia* species assessed, whilst *G. pubiflora* and *G. hillii* were newly discovered to be Mn hyperaccumulator plants. This study also confirms earlier reports of Mn hyperaccumulation in *G. bamagensis*, *G. grayi*, *G. shepherdii*, *G. sankowskyorum*, *G. gonoclada*, *G. bidwillii* [28, 55, 56] and *G. dallachiana*.[37] In classifying plant species as Mn hyperaccumulators, either from chemical surveys of herbarium samples[25, 29, 33, 34, 37], analysing fresh field or experimental material[57, 58]; provenance and within-species variation of the Mn hyperaccumulating trait need to be considered. As evident in all previous analytical data, there is considerable natural

variation among individual plants within a species. In the case of *G. grayi* for example, herbarium data indicated it is not a Mn hyperaccumulator[25], yet a follow-up field study[56] provided contradictory findings. Similarly, *G. lucida* was indicated to be a Mn hyperaccumulator by McLay et al.[37] which is in contrast to the findings of this study. Furthermore, while basic knowledge of Mn movement *in planta* based on crop experiments[10] predicts a positive correlation between leaf age and Mn concentration, the novel physiology of Mn hyperaccumulation may not clearly align with 'normal' plant processes. For example, field studies of Mn hyperaccumulating *G. grayi* and *G. shepherdii* showed Mn concentrations to be greater in young leaves compared to mature leaves.[56] Other sources of variation include geographic effects, genetic variation, rhizosphere soil micro-organisms and/or root exudates that affect soil-Mn mobility.[39, 59] Each of these aforementioned individual factors or various combinations thereof likely underpin intraspecies heterogeneity of Mn hyperaccumulation, whereas interspecies differences are primarily genetic.[60, 61]

The accumulation of Mn, Co and Zn in *G. fragrantissima* confirms previous observations made by Fernando et al. [40] However, the concentrations of Zn (7780 µg g^{-1}) and Co (345 µg g^{-1}) were moderately higher in the previous report [40] compared to this study, whereas Mn levels exceeded their findings. The New Caledonian *Gossia* species, *G. clusioides* subsp. *ploumensis* with up to 10 000 µg g^{-1} Mn[54] and up to 18 000 µg g^{-1} Mn in *Gossia diversifolia* [62], have lower Mn concentrations than some of the newly analysed Australian *Gossia* species. The use of the XRF to chemically screen herbarium specimens has greatly bolstered discovery new hyperaccumulator plants in Southeast Asia[31], New Caledonia[30] and Papua New Guinea.[34]

Leaf-age-related differences in metal concentrations were only statistically significant for foliar Mn in *G. fragrantissima*, which was greater in the older leaves (Fig 3). This is consistent with conventional understanding of Mn phloem mobility[10], but inconsistent with previous field data for Mn hyperaccumulating *G. grayi* and *G. shepherdii*.[56] Analytical distribution maps of metals and other elements across whole-leaf surfaces (Figs 4, 5, 6, 8) capture Mn movement via the xylem, with some apical and marginal accumulation likely due to greater transpiration rates at leaf edges. Inverse Mn and K maps for both species (Figs 5 & 8) match the findings of previous field studies of other Mn-hyperaccumulating species including *Gossia*'s.[57] XFM elemental maps of *G. fragrantissima* leaves (Fig 8) showed similar basal leaf-surface distribution patterns for Mn, Zn and Fe compared to a more widely distributed Co. Leaf Ca accumulation in cell walls was most evident in the leaf venation patterns delineated by thickened walls high in Ca.

This study further confirms that *G. fragrantissima* is a hyperaccumulator of Co, Mn and Zn in a multi-factorial randomised block dosing trial. It accumulates Co, Mn and Zn far above the Co, Mn and Zn hyperaccumulation threshold in young and old leaves, with the highest recorded in old leaves at the highest treatment level. This is in contrast to *G. punctata,* which is not a hyperaccumulator of any of these metals. Older leaves have the highest concentrations of Co, Mn and Zn in *G. fragrantissima* compared to young leaves. Manganese accumulation as observed in *G. fragrantissima* and *G. punctata* suggests that unlike other major nutrient ions whose uptake is generally highly regulated [63], Mn is not similarly tightly controlled.[63-65] Rather, it may have evolved through sequestration mechanisms that detoxify excess tissue Mn, even in non-metallophytes such as certain crop plants including lupins.[66] The higher Co concentration in old leaves of *G. fragrantissima* compared to young leaves may be due to the synergistic effect of Zn on Co uptake as was noted by Palit et al. [67]

Increased Mn uptake observed in the Co+Mn+Zn and in the Co and Zn treatments may be due to the displacement of Mn from anionic functional groups in the presence of Co or Zn as suggested by Irving and Williams. [68] Similar observations have been made for *Odontarrhena chalcidica* treated with Co (Ni+Co and Ni+Co+Mn).[69] These observations offer new insights into metal-ion antagonism and synergism in hyperaccumulators and provide useful baseline information for future studies into transport mechanisms that drive the phenomenon of metal hyperaccumulation.

The XFM analysis showed the presence of elevated Co, Mn and Zn concentrations within the epidermal tissue (cuticle, collenchyma and parenchyma, lower and upper epidermis) with concentrations decreasing in the xylem and phloem in the leaf cross section of *G. fragrantissima* (Fig 7). Metal accumulation in epidermal and sub-epidermal cells of the leaf appears to be a common feature of metal accumulating plants as a similar observation has been found in the Mn hyperaccumulator, *G. exul*.[39] The Zn hyperaccumulator *Noccaea caerulescens* has also been shown to have similar patterns of accumulation[70-72], as have the majority of Ni hyperaccumulator species.[73-77] In contrast, the mesophyll cell has been found to be the Mn sink for *G. bidwillii*.[58] In *G. amplexicaulis* Mn was found to be stored in epidermal layers, the hypodermis and in mesophyll cells[78], and in *Maytenus fournieri* it was accumulated only in the leaf epidermis and multi-layered hypodermis.[39] In this study, high Co, Mn and Zn concentrations in the outer cortical root zone (Fig 9) shows the early stages of uptake. Redistribution through the phloem has also been observed for Ni but not for Co and Mn in other studies.[79-85] This study highlights a new era of hyperaccumulator plants discovery, with the added advantage of identifying species of interest for further ecophysiological and elemental distribution investigation.

Acknowledgements

Farida Abubakari is the recipient of a UQ Graduate School Scholarship (UQGSS) from The University of Queensland. The X-ray fluorescence experiment was undertaken at the Australian Synchrotron (part of ANSTO), Victoria, Australia. We thank Daryl Howard (ANSTO) for support during the synchrotron experiment. This work was supported by the Multi-modal Australian ScienceS Imaging and Visualisation Environment (MASSIVE). The microXRF analysis was undertaken at the Centre for Microscopy and Microanalysis (CMM) at the University of Queensland, Australia.

Author contributions

FA, PNN, PDE, GE and AvdE conducted the glasshouse experiment and collected the samples. AvdE conducted the Desktop and synchrotron XFM experiment. AvdE performed the desktop and synchrotron XFM data processing and analysis. FA collected samples for bulk elemental analysis. FA, PNN, DRF, GKB, PDE, GE and AvdE wrote the manuscript.

Conflicts of interest

There are no conflicts to declare.

Data Availability Statement

The data underlying this article will be shared on reasonable request to the corresponding author.

REFERENCES

1. A. J. M. Baker and R. R. Brooks, Terrestrial higher plants which hyperaccumulate metallic elements. A review of their distribution, ecology and phytochemistry, *Biorecovery.*, 1989, **1**, 81-126.

2. R. D. Reeves, Tropical hyperaccumulators of metals and their potential for phytoextraction, *Plant and Soil*, 2003, **249**, 57-65.

3. A. van der Ent, A. J. M. Baker, R. D. Reeves, A. J. Pollard and H. Schat, Hyperaccumulators of metal and metalloid trace elements: facts and fiction, *Plant and Soil*, 2013, **362**, 319-334.

4. A. J. M. Baker, Accumulators and excluders-strategies in the response of plants to heavy metals, *Journal of plant nutrition*, 1981, **3**, 643-654.

5. A. J. M. Baker, Metal tolerance, *New Phytologist*, 1987, **106**, 93-111.

6. R. D. Reeves, A. J. M. Baker, T. Jaffré, P. D. Erskine, G. Echevarria and A. van der Ent, A global database for plants that hyperaccumulate metal and metalloid trace elements, *New Phytologist*, 2018, **218**, 407-411.

7. R. R. Brooks, *Serpentine and its vegetation: a multidisciplinary approach*, Dioscorides Press, 1987.

8. L. Tiffin, 1977. The form and distribution of metals in plants: an overview. *Biological Implications of Metals in the Environment,* H. Drucker and RE Wildung, Eds., TIC, Oak Ridge, Tennessee, CONF-750929.

9. P. Tinker, Levels, distribution and chemical forms of trace elements in food plants, *Phil. Trans. R. Soc. Lond. B*, 1981, **294**, 41-55.

10. H. Marschner, Mineral Nutrition of Higher Plants Academic Press London Google Scholar, 2002.

11. W. Foulds, Nutrient concentrations of foliage and soil in South-western Australia, *New Phytologist*, 2003, **125**, 529-546.

12. R. D. Reeves, *In: Morel J-L, Echevarria G, Goncharova N (ed) Phytoremediation of metal-contaminated soils, Proceedings of the NATO Advanced Study Institute, Tr˘es˘t' Castle, Czech Republic, 18–30 August 2002, NATO Science Series: IV: Earth and Environmental Sciences 68:25–52.*, Springer, 2006, pp. 25-52.

13. V. Grasmanis and G. Leeper, Toxic manganese in near-neutral soils, *Plant and Soil*, 1966, **25**, 41-48.

14. A. Siman, F. Cradock and A. Hudson, The development of manganese toxicity in pasture legumes under extreme climatic conditions, *Plant and Soil*, 1974, **41**, 129-140.

15. D. Heenan and O. Carter, Tolerance of Soybean Cultivars to Manganese Toxicity 1, *Crop Science*, 1976, **16**, 389-391.

16. R. Gilkes and R. McKenzie, Geochemistry and mineralogy of manganese in soils. In *Manganese in soils and plants*, Springer, 1988, pp. 23-35.

17. J. Hodgson, W. Lindsay and J. Trierweiler, Micronutrient Cation Complexing in Soil Solution: II. Complexing of Zinc and Copper in Displaced Solution from Calcareous Soils 1, *Soil Science Society of America Journal*, 1966, **30**, 723-726.

18. A. Kabata-Pendias and W. Sadurski, Trace elements and compounds in soil, *Elements and their compounds in the environment: Occurrence, analysis and biological relevance*, 2004, 79-99.

19. G. H. Godo and H. Reisenauer, Plant Effects on Soil Manganese Availability 1, *Soil Science Society of America Journal*, 1980, **44**, 993-995.

20. G. W. Leeper and N. C. Uren, Soil science – an introduction, *Melbourne, Australia: Melbourne University Press*, 1997.

21. M. W. Shane and H. Lambers, Manganese accumulation in leaves of *Hakea prostrata* (Proteaceae) and the significance of cluster roots for micronutrient uptake as dependent on phosphorus supply, *Physiologia Plantarum*, 2005, **124**, 441-450.

22. H. Lambers, P. E. Hayes, E. Laliberte, R. S. Oliveira and B. L. Turner, Leaf manganese accumulation and phosphorus-acquisition efficiency, *Trends in Plant Science*, 2015, **20**, 83-90.

23. K. V. DeGroote, G. L. McCartha and A. J. Pollard, Interactions of the manganese hyperaccumulator *Phytolacca americana* L. with soil pH and phosphate, *Ecological Research*, 2016, 1-7.

24. J. Proctor, C. Phillipps, G. Duff, A. Heaney and F. Robertson, Ecological studies on Gunung Silam, a small ultrabasic mountain in Sabah, Malaysia. II. Some forest processes, *The Journal of Ecology*, 1989, 317-331.

25. D. R. Fernando, G. Guymer, R. D. Reeves, I. E. Woodrow, A. J. M. Baker and G. N. Batianoff, Foliar Mn accumulation in eastern Australian herbarium specimens: prospecting for 'new'Mn hyperaccumulators and potential applications in taxonomy, *Annals of Botany*, 2009, **103**, 931-939.

26. T. Jaffré, Accumulation du manganèse par des especes associées aux terrains ultrabasiques de Nouvelle-Calédonie, *Cr Acad. Sci., Paris, D*, 1977, **284**, 1573-1575.

27. T. Jaffré, Accumulation du manganèse par les Protéacées de Nouvelle Calédonie, *Comptes Rendus de l'Académie des Sciences. Série D: Sciences Naturelles*, 1979, **289**, 425-428.

28. S. D. Bidwell, I. E. Woodrow, G. N. Batianoff and J. Sommer-Knudsen, Hyperaccumulation of manganese in the rainforest tree *Austromyrtus bidwillii* (Myrtaceae) from Queensland, Australia, *Functional Plant Biology*, 2002, **29**, 899-905.

29. A. van der Ent, G. Echevarria, A. J. Pollard and P. D. Erskine, X-ray fluorescence ionomics of herbarium collections, *Scientific Reports*, 2019, **9**, 4746.

30. V. Gei, S. Isnard, P. D. Erskine, G. Echevarria, B. Fogliani, T. Jaffré and A. van der Ent, A systematic assessment of the occurrence of trace element hyperaccumulation in the flora of New Caledonia, *Botanical Journal of the Linnean Society*, 2020, **194**, 1-22.

31. P. N. Nkrumah, G. Echevarria, P. D. Erskine and A. van der Ent, Nickel hyperaccumulation in *Antidesma montis - silam*: from herbarium discovery to collection in the native habitat, *Ecological Research*, 2018, **33**, 675-685.

32. A. van der Ent, D. R. Mulligan, R. Repin and P. D. Erskine, Foliar elemental profiles in the ultramafic flora of Kinabalu Park (Sabah, Malaysia), *Ecological Research*, 2018, **33**, 659-674.

33. A. van der Ent, W. J. Przybyłowicz, M. D. de Jonge, H. H. Harris, C. G. Ryan, G. Tylko, D. J. Paterson, A. D. Barnabas, P. M. Kopittke and J. Mesjasz-Przybyłowicz, X-ray elemental mapping techniques for elucidating the ecophysiology of hyperaccumulator plants, *New Phytologist*, 2018, **218**, 432-452.

34. C. Do, F. Abubakari, A. C. Remigio, G. K. Brown, L. W. Casey, V. Burtet-Sarramegna, V. Gei, P. D. Erskine and A. van der Ent, A preliminary survey of nickel, manganese and zinc (hyper) accumulation in the flora of Papua New Guinea from herbarium X-ray fluorescence scanning, *Chemoecology*, 2019, 1-13.

35. S. D. Bidwell, 2000. *Hyperaccumulation of metals in Australian native plants*. PhD Thesis, University of Melbourne.

36. R. D. Reeves, Metal-accumulating plants, *Phytoremediation of toxic metals: using plants to clean up the environment*, 2000.

37. T. McLay, G. D. Holmes, P. I. Forster, S. E. Hoebee and D. R. Fernando, Phylogeny, biogeography and foliar manganese accumulation of *Gossia* (Myrtaceae), *Australian Systematic Botany*, 2019, **31**, 374-388.

38. D. R. Fernando, I. Woodrow, E. Bakkaus, R. Collins, A. J. M. Baker and G. Batianoff, Variability of Mn hyperaccumulation in the Australian rainforest tree *Gossia bidwillii* (Myrtaceae), *Plant and Soil*, 2007, **293**, 145-152.

39. D. R. Fernando, I. Woodrow, T. Jaffré, V. Dumontet, A. T. Marshall and A. J. M. Baker, Foliar manganese accumulation by *Maytenus founieri* (Celastraceae) in its native New Caledonian habitats: populational variation and localization by X-ray microanalysis, *New Phytologist*, 2008, **177**, 178-185.

40. D. R. Fernando, A. T. Marshall, P. I. Forster, S. E. Hoebee and R. Siegele, Multiple metal accumulation within a manganese-specific genus, *American journal of botany*, 2013, **100**, 690-700.

41. G. J. Harden, Taxon concept: C.L. Gross, 1995.

42. N. NPWS, Threatened species of the Upper North Coast of New South Wales–Fauna, *NSW National Parks and Wildlife Service, Northern Directorate, Coffs Harbour*, 2002.

43. U. Kukier and R. L. Chaney, Amelioration of nickel phytotoxicity in muck and mineral soils, *Journal of Environmental Quality*, 2001, **30**, 1949-1960.

44. J. Dai, T. Becquer, J. H. Rouiller, G. Reversat, F. Bernhard-Reversat, J. Nahmani and P. Lavelle, Heavy metal accumulation by two earthworm species and its relationship to total and DTPA-extractable metals in soils, *Soil Biology and Biochemistry*, 2004, **36**, 91-98.

45. W. L. Lindsay and W. A. Norvell, Development of a DTPA soil test for zinc, iron, manganese, and copper 1, *Soil Science Society of America Journal*, 1978, **42**, 421-428.

46. D. Paterson, M. De Jonge, D. Howard, W. Lewis, J. McKinlay, A. Starritt, M. Kusel, C. Ryan, R. Kirkham and G. Moorhead, The X-ray fluorescence microscopy beamline at the Australian synchrotron. *AIP Conference Proceedings*: AIP. 2011**, 219**-222.

47. R. Kirkham, P. Dunn, A. Kuczewski, D. Siddons, R. Dodanwela, G. Moorhead, C. Ryan, G. De Geronimo, R. Beuttenmuller and D. Pinelli, The Maia spectroscopy detector system: engineering for integrated pulse capture, low-latency scanning and real-time processing. *AIP Conference Proceedings*: AIP. 2010, **240**-243.

48. D. Siddons, R. Kirkham, C. Ryan, G. De Geronimo, A. Dragone, A. Kuczewski, Z. Li, G. Carini, D. Pinelli and R. Beuttenmuller, Maia X-ray microprobe detector array system. *Journal of Physics: Conference Series*: IOP Publishing. 2014, 012001.

49. C. Ryan, R. Kirkham, R. Hough, G. Moorhead, D. Siddons, M. De Jonge, D. Paterson, G. De Geronimo, D. Howard and J. Cleverley, Elemental X-ray imaging using the Maia detector array: The benefits and challenges of large solid-angle, *Nuclear Instruments and Methods in Physics Research Section A: Accelerators, Spectrometers, Detectors and Associated Equipment*, 2010, **619**, 37-43.

50. C. Ryan, Quantitative trace element imaging using PIXE and the nuclear microprobe, *International Journal of Imaging Systems and Technology*, 2000, **11**, 219-230.

51. C. Ryan and D. Jamieson, Dynamic analysis: on-line quantitative PIXE microanalysis and its use in overlap-resolved elemental mapping, *Nuclear*

Instruments and Methods in Physics Research Section B: Beam Interactions with Materials and Atoms, 1993, **77**, 203-214.

52. C. Ryan, D. Cousens, S. Sie and W. Griffin, Quantitative analysis of PIXE spectra in geoscience applications, *Nuclear Instruments and Methods in Physics Research Section B: Beam Interactions with Materials and Atoms*, 1990, **49**, 271-276.

53. C. Ryan, B. Etschmann, S. Vogt, J. Maser, C. Harland, E. Van Achterbergh and D. Legnini, Nuclear microprobe–synchrotron synergy: Towards integrated quantitative real-time elemental imaging using PIXE and SXRF, *Nuclear Instruments and Methods in Physics Research Section B: Beam Interactions with Materials and Atoms*, 2005, **231**, 183-188.

54. T. Jaffré, *Étude écologique du peuplement végétal des sols dérivés de roches ultrabasiques en Nouvelle Calédonie*, 1980.

55. D. R. Fernando, A. T. Marshall, P. I. Forster, S. E. Hoebee and R. Siegele, Multiple metal accumulation within a manganese-specific genus, *American Journal of Botany*, 2013, **100**, 690-700.

56. D. R. Fernando, C. S. Smith, M. J. Steinbauer, K. Farnier, S. J. Watson and P. T. Green, Does foliage metal accumulation influence plant–insect interactions? A field study of two sympatric tree metallophytes, *Functional Plant Biology*, 2018, **45**, 945-956.

57. D. R. Fernando, E. Bakkaus, N. Perrier, A. J. M. Baker, I. Woodrow, G. Batianoff and R. Collins, Manganese accumulation in the leaf mesophyll of four tree species: a PIXE/EDAX localization study, *New Phytologist*, 2006, **171**, 751-758.

58. D. R. Fernando, G. N. Batianoff, A. J. M. Baker and I. E. Woodrow, In vivo localization of manganese in the hyperaccumulator *Gossia bidwillii* (Benth.) N. Snow & Guymer (Myrtaceae) by cryo-SEM/EDAX, *Plant, Cell & Environment*, 2006, **29**, 1012-1020.

59. M. Dotaniya and V. Meena, Rhizosphere effect on nutrient availability in soil and its uptake by plants: a review, *Proceedings of the National Academy of Sciences, India Section B: Biological Sciences*, 2015, **85**, 1-12.

60. M. R. Macnair, Within and between population genetic variation for zinc accumulation in *Arabidopsis halleri*, *New Phytologist*, 2002, **155**, 59-66.

61. A. J. Pollard, K. D. Powell, F. A. Harper and J. A. C. Smith, The genetic basis of metal hyperaccumulation in plants, *Critical Reviews in Plant Sciences*, 2002, **21**, 539-566.

62. G. Losfeld, L. L'Huillier, B. Fogliani, S. M. Coy, C. Grison and T. Jaffré, Leaf-age and soil-plant relationships: key factors for reporting trace-elements hyperaccumulation by plants and design applications, *Environmental Science and Pollution Research*, 2015, **22**, 5620-5632.

63. D. T. Clarkson, Factors affecting mineral nutrient acquisition by plants, *Annual review of Plant Physiology*, 1985, **36**, 77-115.

64. D. T. Clarkson, in *Manganese in soils and plants*, Springer, 1988, pp. 101-111.

65. H. Marschner, *Marschner's mineral nutrition of higher plants*, Academic press, 2011.

66. D. R. Fernando and J. P. Lynch, Manganese phytotoxicity: new light on an old problem, *Annals of botany*, 2015, **116**, 313-319.

67. S. Palit, A. Sharma and G. Talukder, Effects of cobalt on plants, *The botanical review*, 1994, **60**, 149-181.

68. H. Irving and R. Williams, Order of stability of metal complexes, *Nature*, 1948, **162**, 746.

69. R. Tappero, E. Peltier, M. Gräfe, K. Heidel, M. Ginder-Vogel, K. Livi, M. L. Rivers, M. A. Marcus, R. Chaney and D. L. Sparks, Hyperaccumulator *Alyssum murale* relies on a different metal storage mechanism for cobalt than for nickel, *New Phytologist*, 2007, **175**, 641-654.

70. M. Vázquez, J. Barceló, C. Poschenrieder, J. Madico, P. Hatton, A. J. M. Baker and G. Cope, Localization of zinc and cadmium in *Thlaspi caerulescens* (Brassicaceae), a metallophyte that can hyperaccumulate both metals, *Journal of Plant Physiology*, 1992, **140**, 350-355.

71. M. Vázquez, C. Poschenrieder, J. Barcelo, A. J. M. Baker, P. Hatton and G. Cope, Compartmentation of zinc in roots and leaves of the zinc hyperaccumulator *Thlaspi caerulescens* J & C Presl, *Botanica Acta*, 1994, **107**, 243-250.

72. H. Küpper, F. J. Zhao and S. P. McGrath, Cellular compartmentation of zinc in leaves of the hyperaccumulator *Thlaspi caerulescens*, *Plant physiology*, 1999, **119**, 305-312.

73. U. Krämer, G. Grime, J. Smith, C. Hawes and A. J. M. Baker, Micro-PIXE as a technique for studying nickel localization in leaves of the hyperaccumulator plant *Alyssum lesbiacum*, *Nuclear Instruments and Methods in Physics Research Section B: Beam Interactions with Materials and Atoms*, 1997, **130**, 346-350.

74. E. Lombi, F. Zhao, S. Dunham and S. McGrath, Cadmium accumulation in populations of *Thlaspi caerulescens* and *Thlaspi goesingense*, *The New Phytologist*, 2000, **145**, 11-20.

75. H. Küpper, E. Lombi, F. J. Zhao, G. Wieshammer and S. P. McGrath, Cellular compartmentation of nickel in the hyperaccumulators *Alyssum lesbiacum*, *Alyssum bertolonii* and *Thlaspi goesingense*, *Journal of Experimental Botany*, 2001, **52**, 2291-2300.

76. J. Mesjasz-Przybylowicz, W. Przybylowicz, D. Rama and C. Pineda, Elemental distribution in *Senecio anomalochrous*, a Ni hyperaccumulator from South Africa, *South African Journal of Science*, 2001, **97**, 593-595.

77. N. P. Bhatia, K. B. Walsh, I. Orlic, R. Siegele, N. Ashwath and A. J. M. Baker, Studies on spatial distribution of nickel in leaves and stems of the metal hyperaccumulator *Stackhousia tryonii* Bailey using nuclear microprobe (micro-PIXE) and EDXS techniques, *Functional plant biology*, 2004, **31**, 1061-1074.

78. D. R. Fernando, A. T. Marshall, B. Gouget, M. Carrière, R. N. Collins, I. E. Woodrow and A. J. M. Baker, Novel pattern of foliar metal distribution in a manganese hyperaccumulator, *Functional Plant Biology*, 2008, **35**, 193-200.

79. L. V. Kochian, Mechanisms of micronutrient uptake and translocation in plants, In *Micronutrients in agriculture*, 1991, 229-296.

80. H. Marschner, Mineral nutrition of higher plants. 2nd, *Edn. Academic Pres*, 1995.

81. V. Page and U. Feller, Selective transport of zinc, manganese, nickel, cobalt and cadmium in the root system and transfer to the leaves in young wheat plants, *Annals of Botany*, 2005, **96**, 425-434.

82. O. Riesen and U. Feller, Redistribution of nickel, cobalt, manganese, zinc, and cadmium via the phloem in young and maturing wheat, *Journal of Plant Nutrition*, 2005, **28**, 421-430.

83. J. Mesjasz-Przybyłowicz, A. Barnabas and W. Przybyłowicz, Comparison of cytology and distribution of nickel in roots of Ni-hyperaccumulating and non-hyperaccumulating genotypes of *Senecio coronatus*, *Plant and Soil*, 2007, **293**, 61.

84. J. Mesjasz-Przybylowicz, W. Przybylowicz, A. Barnabas and A. van der Ent, Extreme nickel hyperaccumulation in the vascular tracts of the tree *Phyllanthus balgooyi* from Borneo, *New Phytologist*, 2016, **209**, 1513-1526.

85. A. van der Ent, D. L. Callahan, B. N. Noller, J. Mesjasz-Przybylowicz, W. J. Przybylowicz, A. Barnabas and H. H. Harris, Nickel biopathways in tropical nickel hyperaccumulating trees from Sabah (Malaysia), *Scientific reports*, 2017, **7**, 41861.

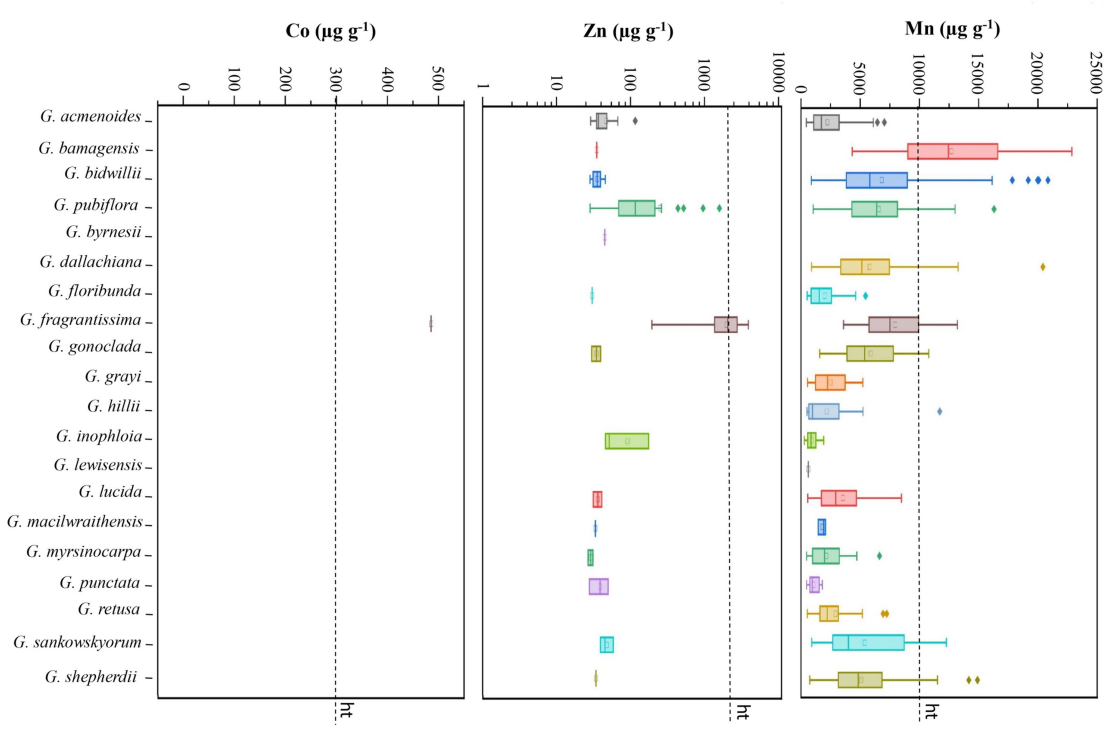

Figure 1. Cobalt, Zn and Mn accumulation in the genus *Gossia* revealed by systematic assessment of all the *Gossia* specimens at the Queensland Herbarium by the use of the X-ray Florescence Spectroscopy. Concentration values of Co, Zn and Mn are in µg g^{-1}. ht is the hyperaccumulation threshold of Co (300 µg g^{-1}), Zn (3000 µg g^{-1}) and Mn (10 000 µg g^{-1}). Keys to symbol of boxplots: open squares are the 25% to 75% quartiles, lines within the boxes indicates the median whereas the whiskers mark the maximum and minimum values and circles are outliers. Values below the limit of detection (LOD) were excluded.

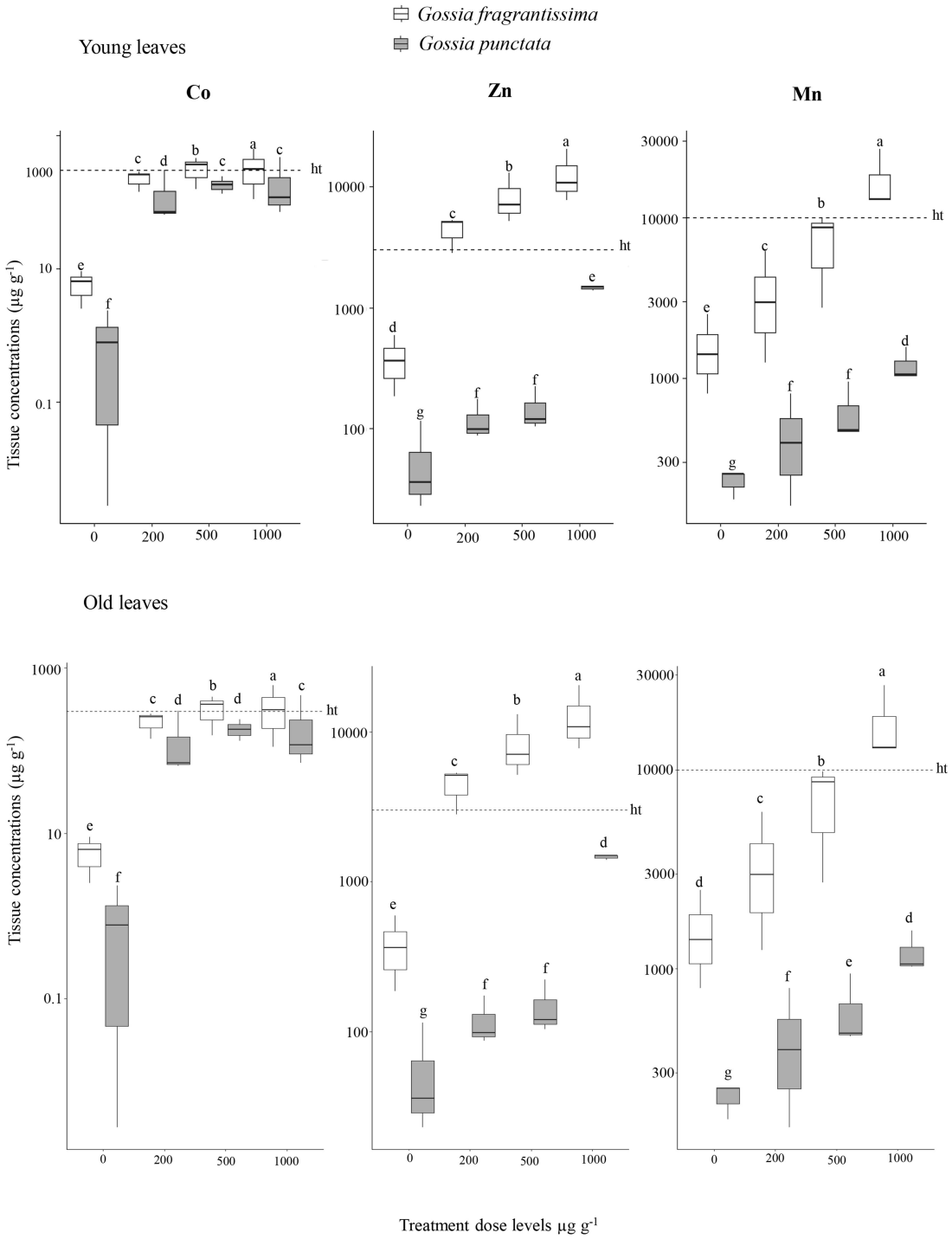

Figure 2. Cobalt, Zn and Mn concentrations in young and old leaves of *Gossia fragrantissima* and *Gossia punctata* after exposure to different levels of Co, Mn and Zn treatments. Values are average of three replicates ± standard error. ht is the hyperaccumulation threshold of Co (300 µg g^{-1}), Zn (3000 µg g^{-1}) and Mn (10 000 µg g^{-1}).

Keys to symbol of boxplots: open squares are the 25% to 75% quartiles, lines within the boxes indicates the median whereas the whiskers mark the maximum and minimum values and circles are outliers. Mean ± standard error followed by the same letter are not significantly different (p <0.05) as stated by Duncan-Waller K-ratio t-test.

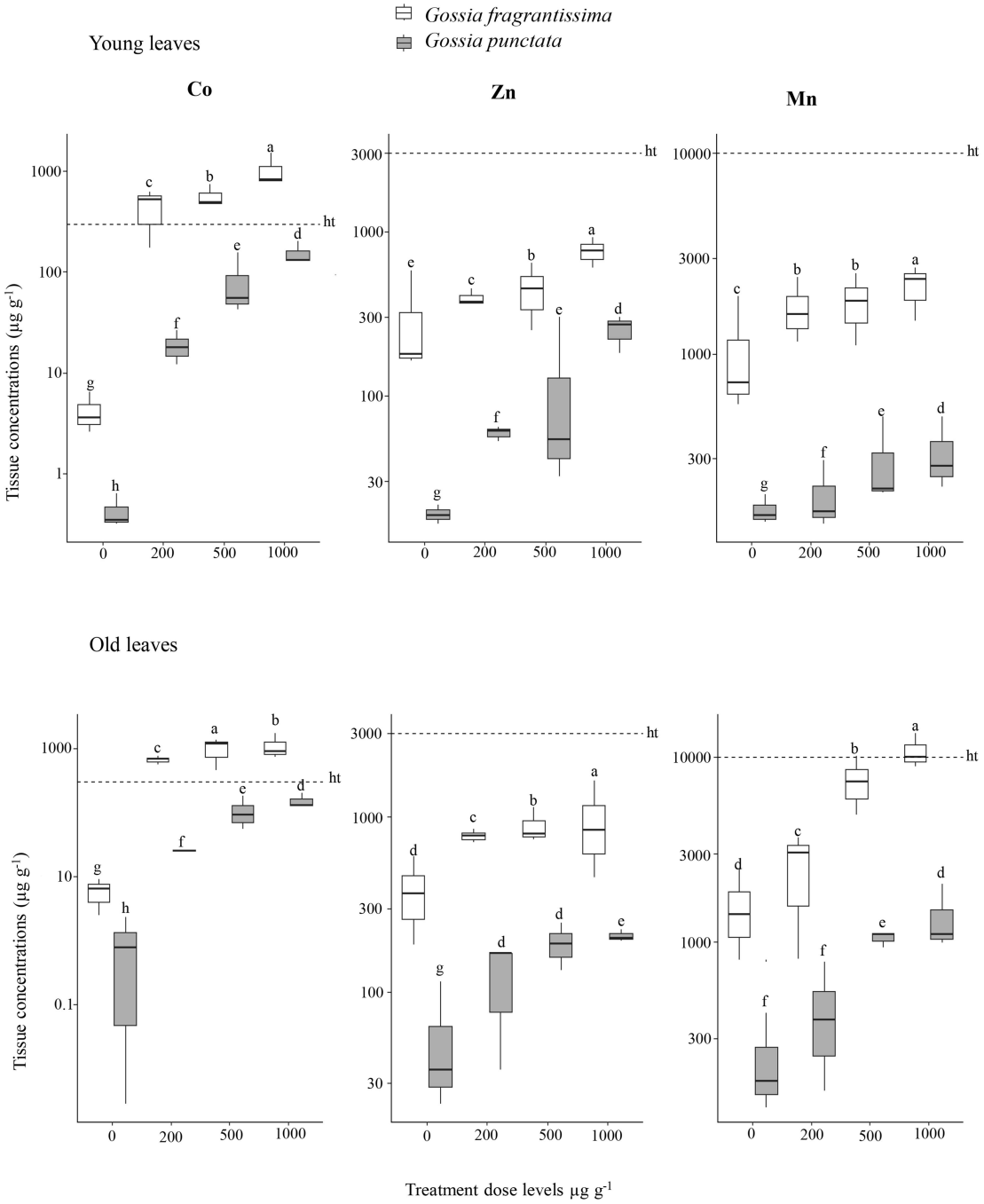

Figure 3. Cobalt, Zn and Mn concentrations in young and old leaves of *Gossia fragrantissima* and *Gossia punctata* after exposure to different combinations of Co+Mn+Zn treatments. Values are average of three replicates ± standard error. ht is the hyperaccumulation threshold of Co (300 µg g^{-1}), Zn (3000 µg g^{-1}) and Mn (10 000 µg g^{-1}). Keys to symbol of boxplots: open squares are the 25% to 75% quartiles, lines within the boxes indicates the median whereas the whiskers mark the maximum and minimum values

and circles are outliers. Mean ± standard error followed by the same letter are not significantly different (p <0.05) as stated by Duncan-Waller K-ratio t-test.

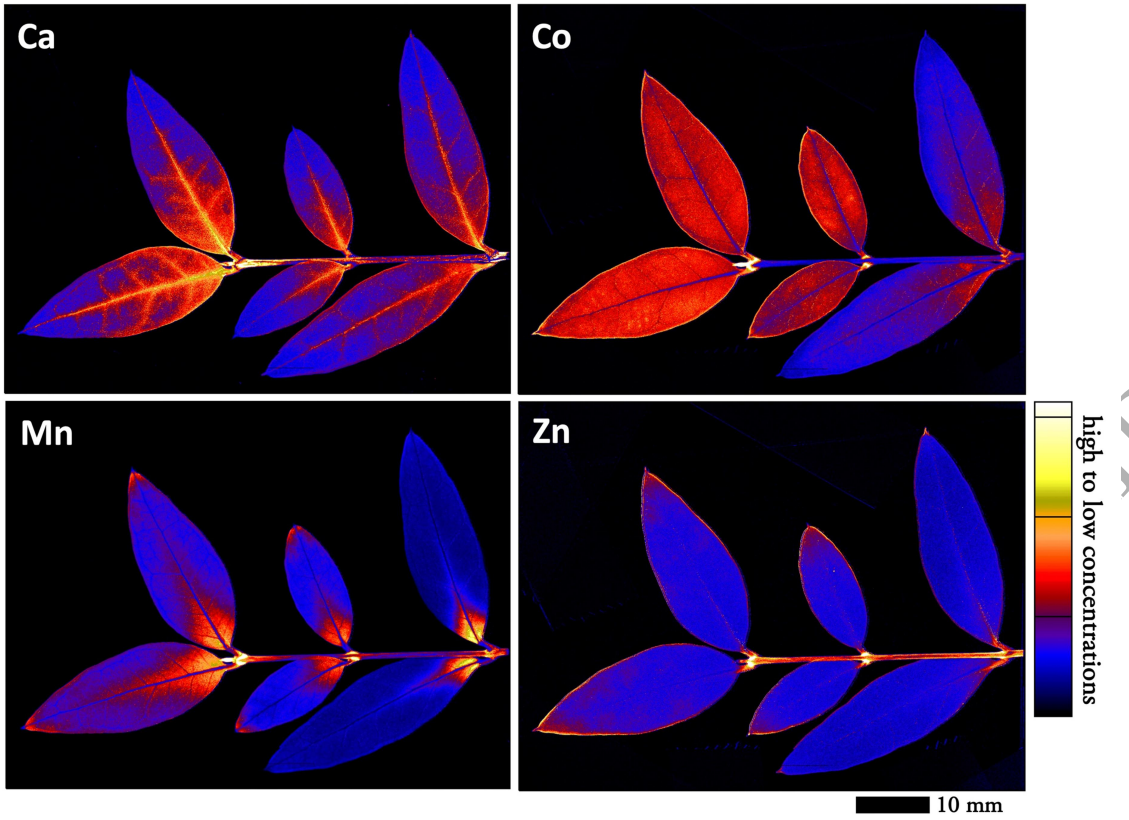

Figure 4. Laboratory μXRF maps of Ca, Co, Mn and Zn of intact terminal branch of *Gossia fragrantissima*.

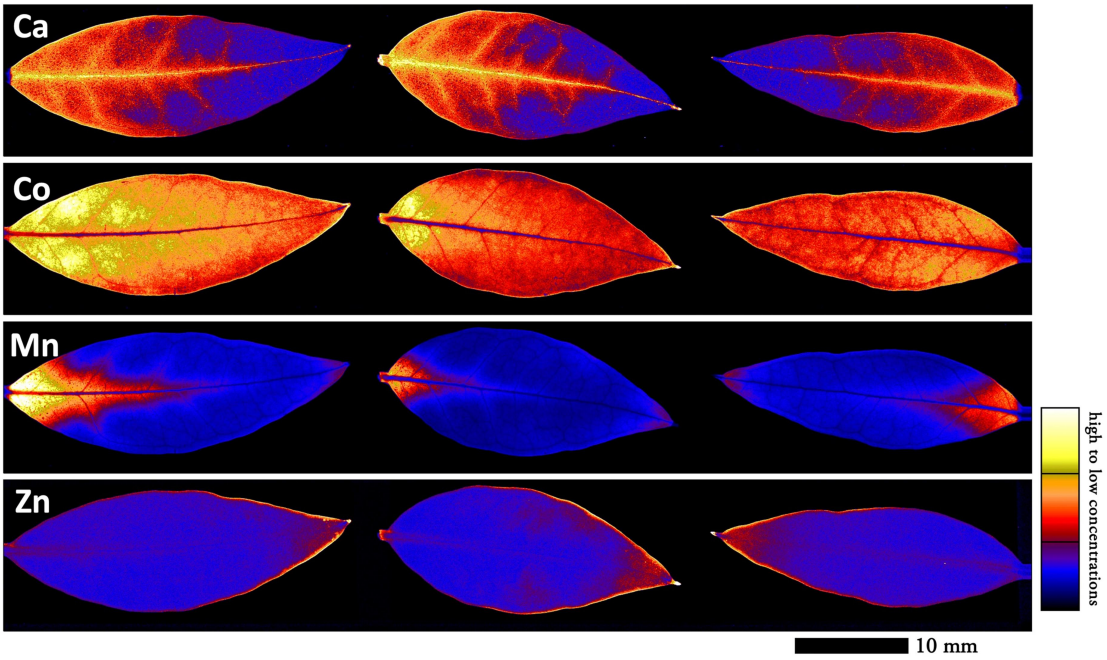

Figure 5. Laboratory μXRF maps of Ca, Co, Mn and Zn of whole leaves (old to young leaves from left to right) of *Gossia fragrantissima.*

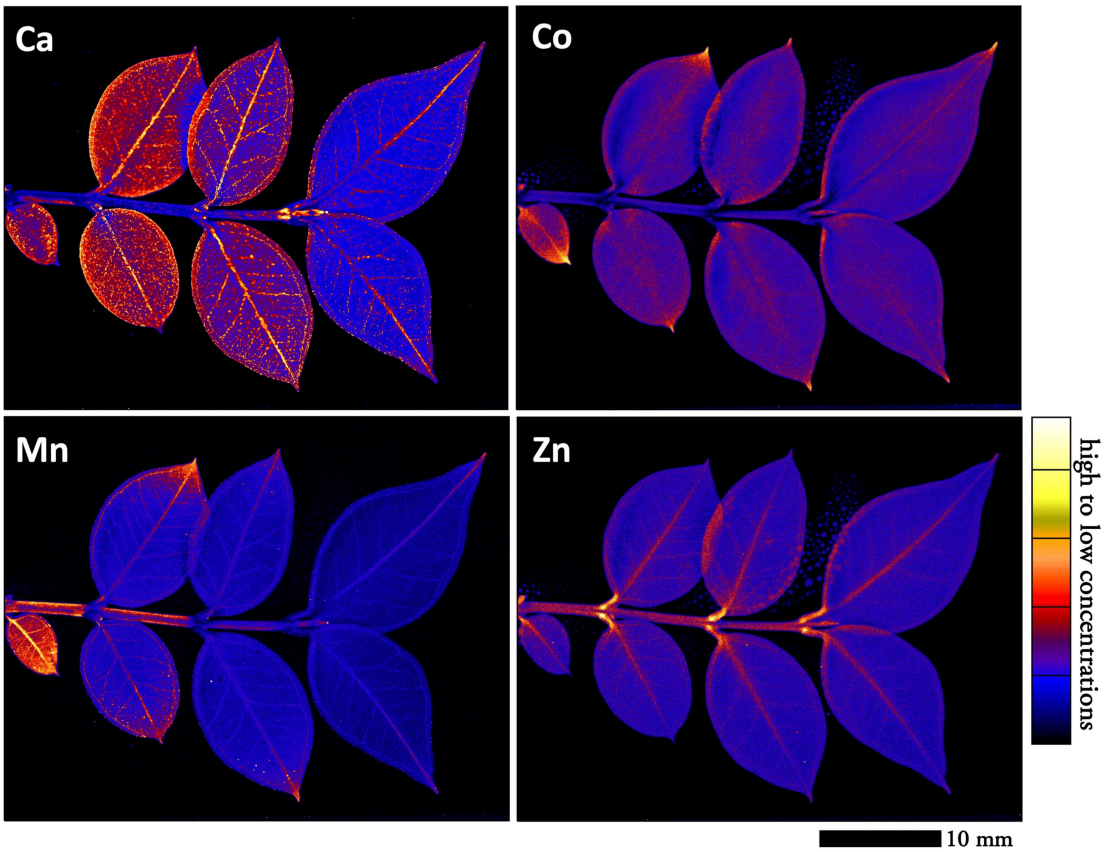

Figure 6. Laboratory μXRF maps of Mn, Ca, Co, Mn and Zn of intact terminal branch of *Gossia punctata.*

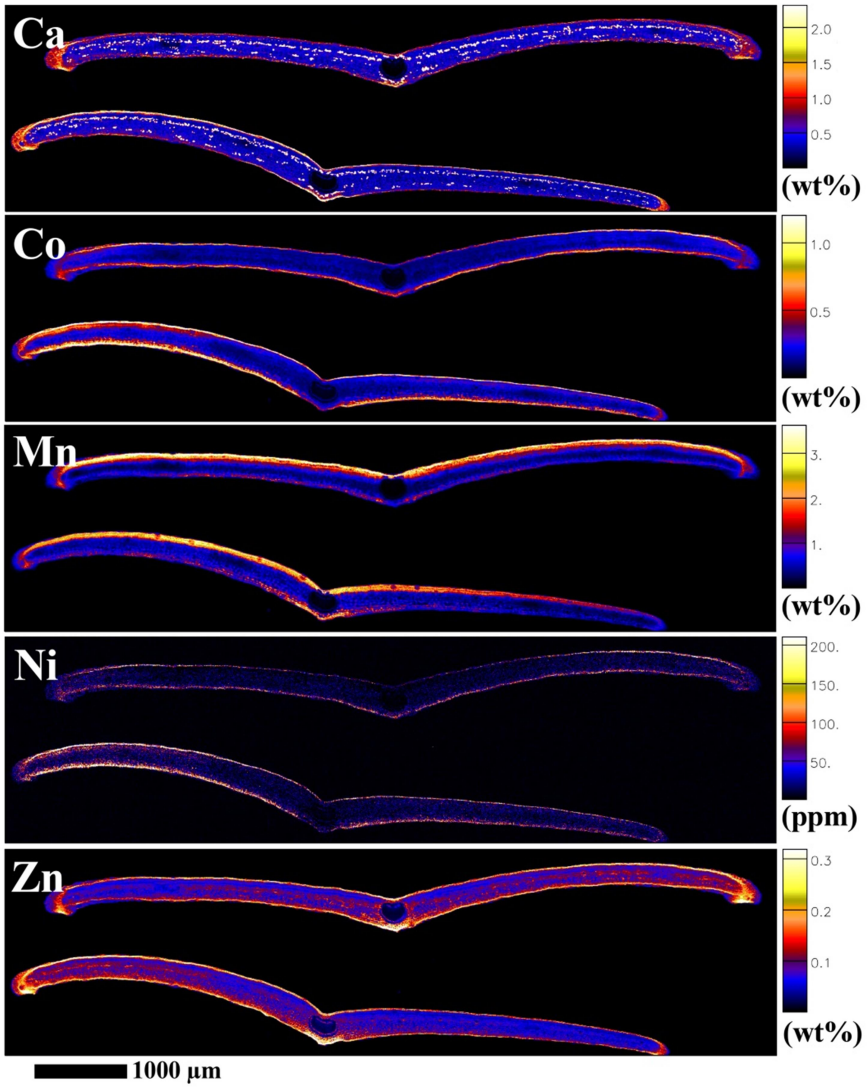

Figure 7. Synchrotron µXRF maps (Ca, Co, Mn, Ni and Zn) of leaf cross-section of *G. fragrantissima.* Concentration scale in wt% dry weight or in µg g^{-1} dry weight. Scale bar 1000 µm.

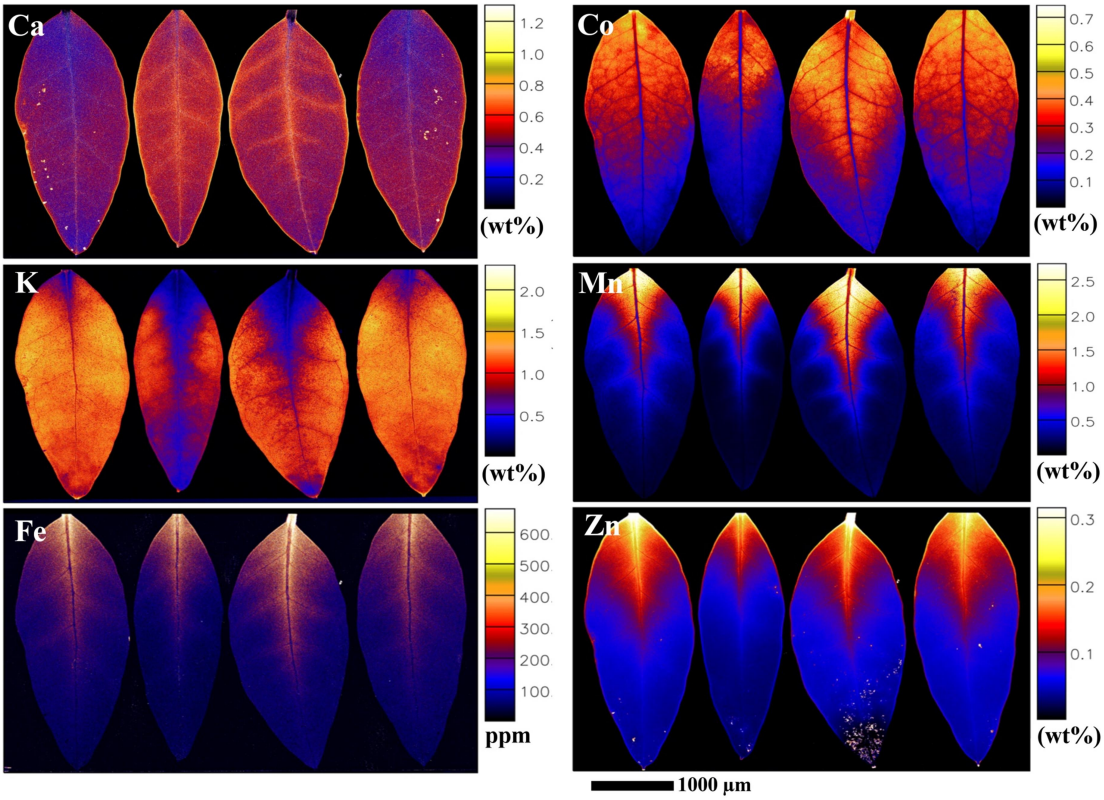

Figure 8. Synchrotron µXRF maps (Ca, K, Fe, Co, Mn, Zn) of whole *Gossia fragrantissima* leaves (all mature leaves of approximately the same age). Concentration scale in wt% dry weight or in µg g^{-1} dry weight. Scale bar 1000 µm.

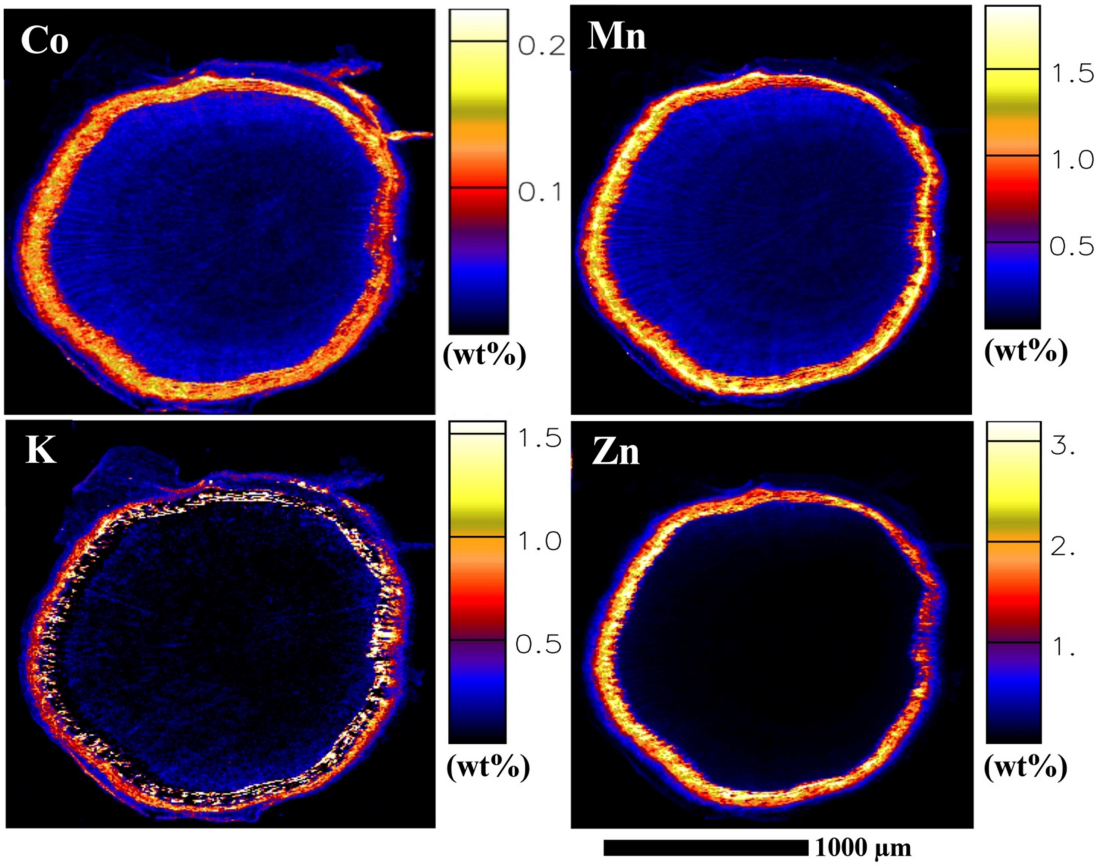

Figure 9. Synchrotron µXRF maps (Co, Mn, K, Zn) of root-cross section of *Gossia fragrantissima.* Concentration scale in wt% dry weight or in µg g^{-1} dry weight. Scale bar 1000 µm.